

# Relaxation Oscillator Using Superconducting Schmitt Trigger Inverter

Takeshi Onomi<sup>†</sup>

<sup>†</sup>Research Institute of Electrical Communication, Tohoku University  
 2-1-1 Katahira, Aoba-ku, Sendai 980-8577, Japan  
 Email: onomi@riec.tohoku.ac.jp

**Abstract**– A new superconducting Schmitt trigger inverter and a relaxation oscillator are proposed. The proposed superconducting Schmitt trigger inverter is composed of a threshold gate using coupled superconducting interference devices (SQUIDs). The oscillator is based on the concept using a Schmitt trigger inverter and a delayed feedback loop. It is shown that the inverter with an inductive feedback loop can operate as the relaxation oscillator by a numerical simulation. We also show that the relaxation oscillator with an additional buffer gate generates a square waveform.

## 1. Introduction

A Schmitt trigger is a famous threshold element with hysteretic characteristics[1]. Semiconductor threshold gates with such characteristics are widely used for some popular applications such as hysteretic comparators or simple oscillators. In this paper, we report a new superconducting Schmitt trigger circuit and a relaxation oscillator using the Schmitt trigger inverter. The Schmitt trigger inverter consists of a threshold gate with hysteretic characteristics using two coupled superconducting interference devices (c-SQUIDs) gates with a cascade connection[2]. We also discuss a relaxation oscillator using the proposed superconducting Schmitt trigger. Some superconducting relaxation oscillators have been already proposed[3]-[6]. These oscillators were based on hysteresis properties of switching characteristics of one or two Josephson junctions shunted by a series of inductance and resistance. It is expected that our new relaxation oscillator has high design flexibility and stability due to its well-defined threshold characteristics. Moreover, we also propose that the relaxation oscillator with an additional output buffer gate can operate as a square waveform generator. The square waveform generator is valuable in a clock generator of superconducting logic circuits or sensor devices operating at the low temperature environment.

## 2. Schmitt Trigger Circuit Using Coupled SQUIDs Gate with Flat Output Characteristics

We use JSIM[7] for circuit simulations with Nb/AlOx/Nb Josephson junctions with critical current density  $J_c = 2.5 \text{ kA/cm}^2$ . The parameter of  $J_c$  is set on the assumption that the circuits will be fabricated in the clean room for analog-digital superconductivity (CRAVITY) of

National Institute of Advanced Industrial Science and Technology with the standard process 2 (STP2) [8].

### 2.1. Coupled SQUIDs Gate with Flat Output Characteristics

We have proposed a superconducting threshold gate with flat output characteristics[2]. Figure 1 shows the circuit diagram of the gate composed of cascaded two-stage c-SQUIDs gate. The double-junction SQUID (DC-SQUID) reads out the quantum state of the single-junction SQUID[9]. Because the transition of the quantum state of the single-junction SQUID follows a step-like function, the output voltage of the DC-SQUID is characterized by a sharp rise in voltage. We have proposed a neural network using this characteristic corresponding to a sigmoid-shaped function which is typical for generating neuron output[10].

Figure 2 shows a typical static input vs. output characteristics of the threshold gate. Although the output of the first stage c-SQUIDs gate  $V_{out1}$  has a round shape at a vicinity of the rising edge as shown in Fig. 2, that of the second one  $V_{out2}$  has the flat shape. The quantum state of the single-junction SQUID ( $J_1, L_1 - L_4$ ) corresponds to the number of flux-quanta in the loop. When a negative input

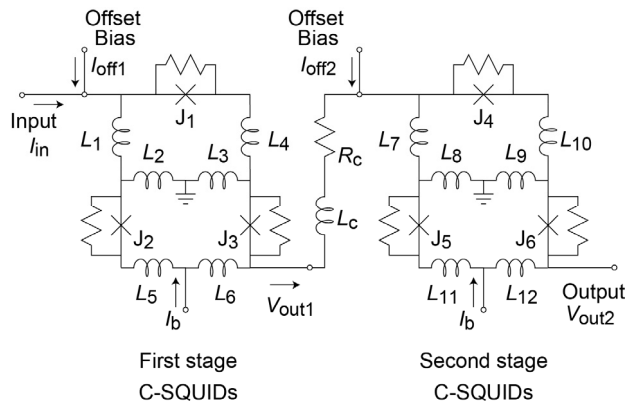


Figure 1: Threshold gate composed of cascaded two-stage c-SQUIDs gate. The device parameters are designed as  $I_{c1} = 0.150 \text{ mA}$ ,  $I_{c2} = I_{c3} = I_{c5} = I_{c6} = 1.50 \text{ mA}$ ,  $I_{c4} = 0.220 \text{ mA}$ ,  $L_1 = 1.32 \text{ pH}$ ,  $L_2 = L_3 = L_8 = L_9 = 1.13 \text{ pH}$ ,  $L_4 = L_{10} = 0.40 \text{ pH}$ ,  $L_5 = L_6 = L_{11} = L_{12} = 0.34 \text{ pH}$ ,  $L_7 = 1.20 \text{ pH}$ ,  $L_c = 10.0 \text{ pH}$ ,  $R_c = 0.10 \text{ } \Omega$ ,  $I_{off1} = 0.50 \text{ mA}$ ,  $I_b = 2.85 \text{ mA}$ . ( $I_{cX}$  denotes Josephson critical current value of the junction  $J_X$ .)

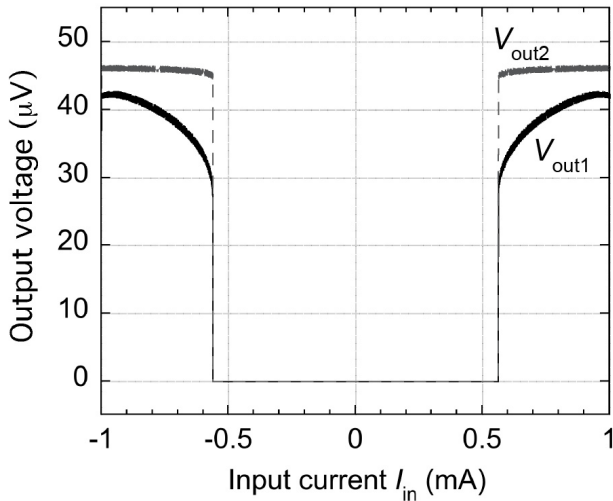


Figure 2: Simulated static input vs. output characteristics of the threshold gate. ( $I_{\text{off1}} = 0.0$  mA,  $I_{\text{off2}} = 0.50$  mA) The output voltage  $V_{\text{out1}}$  and  $V_{\text{out2}}$  denote the output of the first stage c-SQUIDs and that of the second one, respectively.

current over the threshold is supplied, the quantum state transits from “0” to “-1” state, e.g., a negative flux quantum is inserted in the loop. However, the polarity of the output voltage does not depend on the direction of the flux. Hence, the static input vs. output characteristics is symmetrical about the y-axis as shown in Fig.2. This feature is useful for creating an inverting configuration of the threshold characteristics.

## 2.2. Superconducting Schmitt Trigger

To obtain the characteristics with Schmitt trigger shape, the input gate must have the hysteretic characteristics. Because the output voltage transitions are decided by the quantum states of the single-junction SQUID ( $J_1, L_1 - L_4$ ), the hysteretic property of the quantum state in the single-junction SQUID is required for making the hysteretic output characteristics. To obtain such characteristics,  $LI_c$  product of the single-junction SQUID is just increased.

Figure 3 shows a static input vs. output characteristics as the Schmitt trigger. The critical current of the junction  $J_1$  is designed as  $I_{c1} = 0.188$  mA, which is larger than the original parameter, to obtain a large  $LI_c$  product. Other circuit parameters are the same as those described in Fig. 1. The output  $V_{\text{out2}}$  shows an identical characteristics for the Schmitt trigger.

## 2.3. Superconducting Schmitt Trigger Inverter

A comparator-based Schmitt trigger is used in its inverting configuration for a simple relaxation oscillator. It is not so difficult to obtain the inverting configuration of the Schmitt trigger mentioned in the previous section.

A negative offset bias current  $I_{\text{off1}}$  is supplied to the first stage c-SQUID gate to achieve such an inverting configuration. As shown in Fig. 2, the polarity of the output voltage of the threshold gate does not depend on that of the input current. Therefore, the inverting configuration is achieved by the region of the input current ensuring “-1” and “0” of the quantum states.

Figure 4 shows a static input vs. output characteristics as the Schmitt trigger inverter. The output  $V_{\text{out2}}$  shows an identical characteristics for the Schmitt trigger inverter. In the next section, we discuss a relaxation oscillator using this Schmitt trigger inverter and a feedback element.

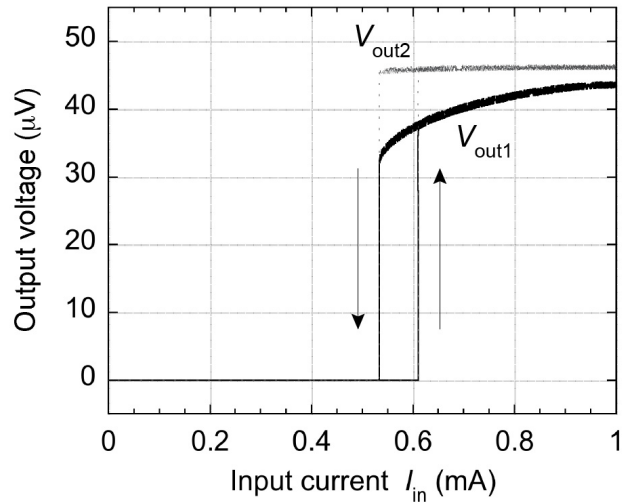


Figure 3: Simulated static input vs. output characteristics as the Schmitt trigger. ( $I_{\text{off1}} = 0$  mA,  $I_{\text{off2}} = 0.50$  mA) The critical current of the junction  $J_1$  is designed as  $I_{c1} = 0.188$  mA. Other circuit parameters are the same as those described in Fig. 1.

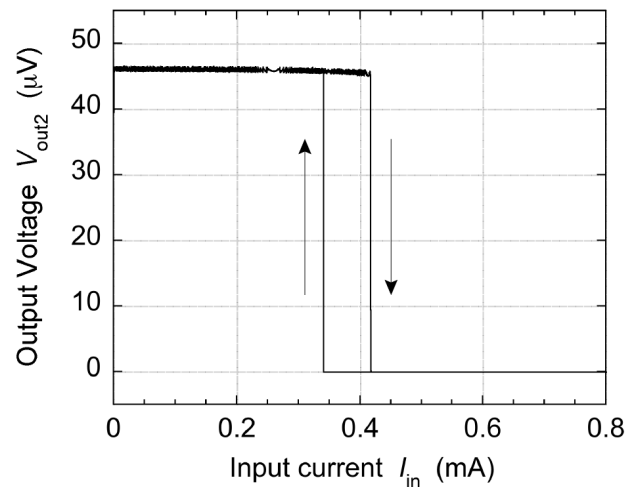


Figure 4: Simulated static input vs. output characteristics as the Schmitt trigger Inverter. ( $I_{\text{off1}} = -0.88$  mA,  $I_{\text{off2}} = 0.50$  mA)

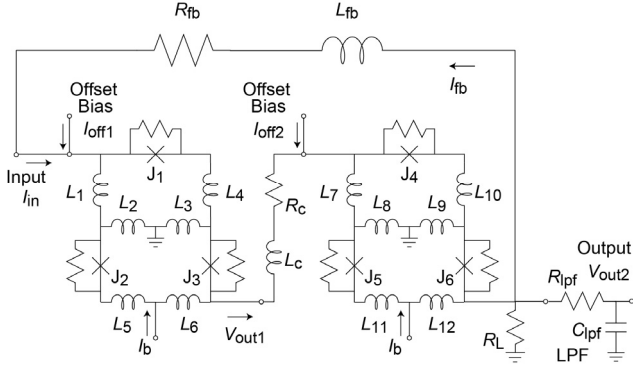


Figure 5: Relaxation oscillator using the superconducting Schmitt trigger inverter. The device parameters are designed as  $I_{c1} = 0.188$  mA,  $L_{fb} = 5.0$  nH,  $R_{fb} = 0.10$   $\Omega$ ,  $R_L = 0.50$   $\Omega$ ,  $R_{lpf} = 1.0$  k $\Omega$ ,  $C_{lpf} = 0.10$  pF,  $I_{off1} = -0.88$  mA. Other circuit parameters are the same as those described in Fig. 1. The passive low pass filter composed of  $R_{lpf}$  and  $C_{lpf}$  is connected to the output of the relaxation oscillator to remove the high frequency spectrum due to Josephson oscillation.

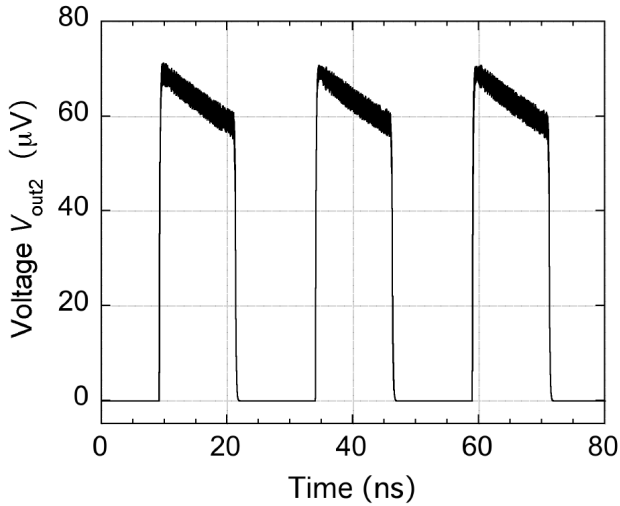


Figure 6: A simulated output waveform of the relaxation oscillator using the superconducting Schmitt trigger inverter.

### 3. Relaxation Oscillator Using Superconducting Schmitt Trigger Inverter Circuit

#### 3.1. Relaxation Oscillator Using Superconducting Schmitt Trigger Inverter and Feedback Elements

It is well known that a circuit composed of the Schmitt trigger and some negative feedback element operates as a simple relaxation oscillator. Using the semiconductor circuits, this is achieved by connecting a single RC integrating circuit between the output and the input of an inverting Schmitt trigger[11]. A typical delay element in the superconducting electronics is usually provided by

some combinations of a resistance and an inductance. We propose a relaxation oscillator using the superconducting Schmitt trigger inverter and a delay element using a series of the resistance  $R_{fb}$  and the inductance  $L_{fb}$  as shown in Fig. 5. A passive low pass filter composed of  $R_{lpf}$  and  $C_{lpf}$  is connected to the output of the relaxation oscillator to remove the high frequency spectrum due to Josephson oscillation. This low pass filter does not effect to the operation of the relaxation oscillator substantially, because the resistance  $R_{lpf}$  is rather large compared to the load resistance  $R_L$ .

Figure 6 shows a simulated output waveform of the relaxation oscillator using the superconducting Schmitt trigger inverter. It is confirmed that periodical pulse trains are generated.

Unfortunately, this oscillator is not able to generate an ideal square waveform because of the load variation caused by  $LR$  feedback loop. The feedback current  $I_{fb}$  increases logarithmically after the gate switches from zero to a voltage state. This brings about the decrease of the output voltage because a part of the bias current  $I_b$  of the second stage c-SQUIDs flows forward the feedback loop. Hence, the output voltages of the pulses does not become flat. To avoid this drawback, we introduce an output buffer gate in the next subsection.

#### 3.2. Relaxation Oscillator with Output Buffer Gate

We introduce an additional output buffer gate to the output of the relaxation oscillator proposed in the previous section. Figure 7 shows a circuit diagram of the relaxation oscillator with an output buffer gate. Introducing this output buffer gate brings about the effect of decreasing the output variation due to the existence of the feedback loop. Figure 8 shows a simulated oscillation waveform of the relaxation oscillator with the output buffer gate. We can confirm that output voltages of the pulses are flat compared to the oscillator without the output buffer.

The proposed new relaxation oscillator is able to generate the square waveform easily. The oscillation frequency of the oscillator can be easily changed by adjusting the inductance of delay element  $L_{fb}$ . Moreover, the duty cycle can be changed by adjusting the threshold of the Schmitt trigger (adjusting the offset bias current  $I_{off1}$ ). We have not investigated details of the circuit parameter dependence of these variable parameters as the square waveform generator yet. These investigations will be reported in near future.

We have already reported a fabricated threshold gate using cascaded two-stage c-SQUIDs gate[2]. It is not so difficult to design the proposed oscillator using Schmitt trigger inverter, because the basic structure of the inverter is the same as the previously fabricated gate. We suppose the square waveform generator is valuable in a clock generator of superconducting logic circuits or sensor devices operating at the low temperature environment.

### 4. Conclusion

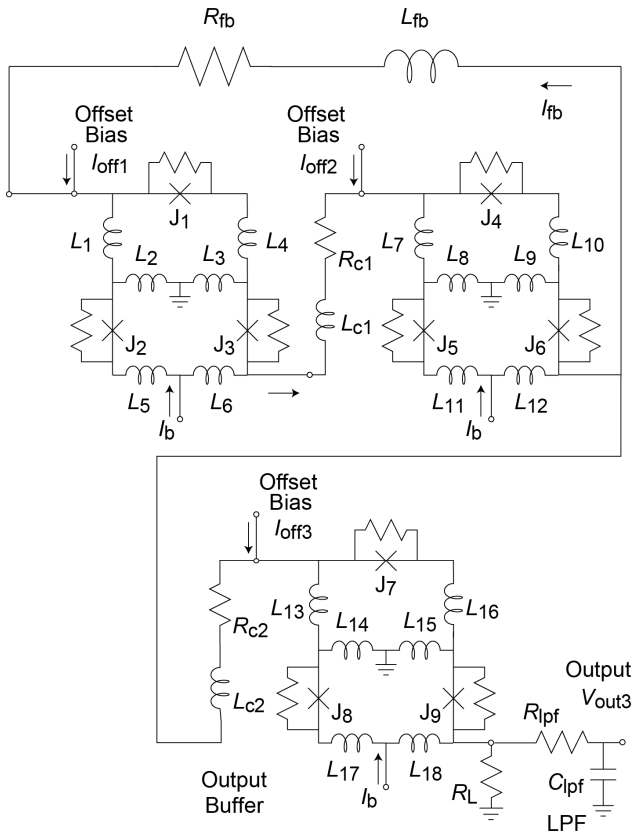


Figure 7: Relaxation oscillator with an output buffer gate using the superconducting Schmitt trigger inverter. The device parameters are designed as  $I_{c1} = 0.188$  mA,  $L_{fb} = 5.0$  nH,  $R_{fb} = 0.40$   $\Omega$ ,  $I_{c7} = 0.220$  mA,  $I_{c8} = I_{c9} = 1.50$  mA,  $L_{13} = 1.20$  pH,  $L_{14} = L_{15} = 1.13$  pH,  $L_{16} = 0.40$  pH,  $L_{17} = L_{18} = 0.34$  pH,  $L_{c2} = 10.0$  pH,  $R_{c2} = 0.20$   $\Omega$ ,  $R_L = 0.10$   $\Omega$ ,  $R_{lpf} = 1.0$  k $\Omega$ ,  $C_{lpf} = 0.10$  pF,  $I_{off1} = -0.88$  mA,  $I_{off3} = 0.50$  mA. Other circuit parameters are the same as those described in Fig. 1.

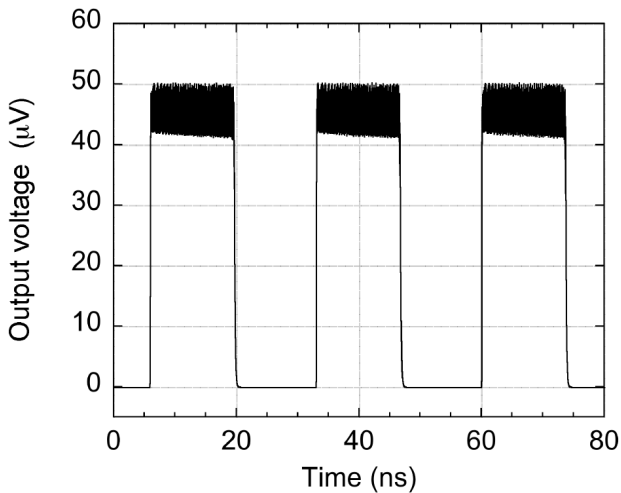


Figure 8: A simulated oscillation waveform in the relaxation oscillator with the output buffer gate.

We proposed a new superconducting Schmitt trigger inverter and a relaxation oscillator using the inverter with the feedback element. The proposed superconducting Schmitt trigger inverter was designed using a coupled SQUIDs threshold gate, and its operation was confirmed numerically. It was shown that the Schmitt trigger inverter with an inductive feedback loop can operate as the relaxation oscillator by a numerical simulation. We also confirmed that the relaxation oscillator with an additional buffer gate generates a square waveform.

### Acknowledgments

This research was supported by JSPS KAKENHI Grant Number 24500271.

### References

- [1] O. H. Schmitt, "A thermionic trigger," *J. Sci. Instrum.*, vol.15, pp. 24-26, 1938.
- [2] T. Onomi and K. Nakajima, "Neuron Circuit using Coupled SQUIDs Gate with Flat Output Characteristics for Superconducting Neural Network," *IEICE Trans. Electron.*, vol. E97-C, no. 3, pp. 173–177, March 2014.
- [3] J. E. Zimmerman and A. H. Silver, "Coherent radiation from high-order quantum transitions in small-area superconducting contacts," *Phys. Rev. Lett.*, vol. 19, no. 1, pp. 14-16, Jul. 1967.
- [4] F. L. Vernon and R. J. Pedersen, "Relaxation oscillations in Josephson junctions," *J. Appl. Phys.*, vol. 39, no. 6, pp. 2661-2664, May 1968.
- [5] N. Calander, T. Claeson, and S. Rudner, "A subharmonic Josephson relaxation oscillator – amplification and locking," *Appl. Phys. Lett.*, vol. 39, no. 6, pp. 504-506, Sep. 1981.
- [6] Y. Mizugaki, "Numerical demonstration of relaxation oscillation in a resistive superconducting quantum interference device with two nonhysteretic Josephson junctions," *IEEE Trans. Appl. Superconduct.*, vol. 20, no. 5, pp. 2322–2326, Oct. 2010.
- [7] E. S. Fang and T. Van Duzer, "A Josephson integrated circuit simulator (JSIM) for superconductive electronics application," *Ext. Abst. 1989 Int. Superconductivity Conf.*, pp.407-410, June 1989.
- [8] H. Numata and S. Tahara, "Fabrication technology for Nb integrated circuits," *IEICE Trans. Electron.*, vol. E84-C, no. 1, pp. 2–8, Jan. 2001.
- [9] Y. Mizugaki, K. Nakajima, Y. Sawada, and T. Yamashita, "Implementation of new superconducting neural circuits using coupled SQUIDs," *IEEE Trans. Appl. Superconduct.*, vol. 4, no. 1, pp. 1–8, March 1994.
- [10] T. Onomi, M. Maenami and K. Nakajima, "Superconducting Neural Network for Solving a Combinatorial Optimization Problem," *IEEE Trans. Appl. Superconduct.*, vol. 21, no. 3, pp. 701–704, June 2011.
- [11] For example: Data sheet of MM74C14 Hex Schmitt Trigger, Fairchild Semiconductor Co..